Binary ORC (organic Rankine cycles) power plants for the exploitation of medium–low temperature geothermal sources – Part A: Thermodynamic optimization

Marco Astolfi*, Matteo C. Romano, Paola Bombarda, Ennio Macchi

Politecnico di Milano, Energy Department, via Lambruschini 4, 20156 Milano, Italy

Received 17 May 2013
Received in revised form
14 October 2013
Accepted 20 November 2013
Available online 10 January 2014

1. Introduction

The increasing attention to pollutants and greenhouse gases emission from the power generation sector and the concerns about fossil fuels supply and price have been leading to a massive growth of those technologies that can produce electric energy from renewable sources and waste heat recovery. Nowadays, favorable feed-in tariffs and other financial incentives make competitive the exploitation of renewable sources and low-grade heat for power production in many countries. For this reason, renewable sources and energy efficiency have been receiving an increasing interest in the power generation sector. In this context, the exploitation of heat from a wide variety of sources, like hot geothermal brines, biomass, sun and exhaust gases from engines and industrial processes is certainly one of the most promising options.

While steam cycles will probably remain the only competitive technology for large scale heat recovery and external combustion cycles for power generation, their application in small scale units and for low grade heat utilization, typical of many renewable sources, has a number of drawbacks. In these applications, the use of organic working fluids in Rankine cycles can be preferable vs. steam for a number of reasons:

- A favorable "shape" of the thermodynamic cycle, allowing for high cycle and heat recovery efficiencies, achievable by simple cycle layouts (no vapor superheating, no reheating, no multiple regenerative bleedings from the turbine) [1].
- Reasonable volume flow rates and low enthalpy drops in the turbine. These points allow for a favorable turbine design, resulting in high isentropic efficiencies with a limited number of stages (even a single one), a reasonable size and hence competitive manufacturing costs [1].
- Favorable operating conditions for the turbine, with low mechanical stresses due to the low peripheral speeds, no blade erosion issues due to the dry expansion (no droplets formation during fluid expansion even without superheating).
- Possibility of adopting lower maximum pressure and cost of the high pressure components in case of medium–high temperature heat sources.

* Corresponding author. Tel.: +39 (0)2 2399 3935.
E-mail address: marco.astolfi@mail.polimi.it (M. Astolfi).

Table 1
Review of the works in the literature on ORC optimization.

Reference	Heat source	Available thermal input[a] or power output	Types of cycles	Considered fluids	Machines efficiencies	Fixed variables	Optimization variables	Optimization function	Component sizing	Optimal cycles
Invernizzi, Bombarda (1997) [11]	Geothermal brine @ 100–300 °C	–	Sub-SA rec/no-rec	R11, R114, R245ca, R245fa, R236fa, R134a, HFE-245fa, n-butane, n-pentane, n-perfluoro-pentane	$\eta_{is,turb} = 75\%$ $\eta_{wf,pump} = 50\%$	$\Delta T_{pp,PHE} = 20$ °C $\Delta T_{sh} = 10$ °C $\Delta T_{pp,rec} = 20$ °C $T_{cond} = 40$ °C $\Delta p_i = 0$	p_{eva}	Plant exergy efficiency	–	–
Hettiarachchi, Golubovic, al. (2007) [12]	Geothermal brine @ 70–90 °C	10 MW_{el}	Sub-SA no-rec	PF 5050, R123, NH_3, n-pentane	$\eta_{is,turb} = 85\%$ $\eta_{wf,pump} = 75\%$ $\eta_{mec-el} = 96\%$ $\eta_{cw,pump} = 80\%$	$T_{cw} = 30$ °C Δp_i = calc	T_{eva} T_{cond} u_{geo} u_{cw}	Specific heat exchange area: m^2/kW	Heat exchangers area	*NH_3:* $T_{eva} = 76.9$ °C $T_{cond} = 43.0$ °C $\eta_{cycle} = 8.9\%$ $\eta_{plant} = 8.0\%$[a] $\alpha = 0.34$ m^2/kW
Invernizzi et al. (2007) [3]	WHR: MGT flue gas @ 250–350 °C	–	Sub-SA rec	HFC-43-10mee, HCFC-123, n-Pentane, CFC-113, 2-2-Dimethylbutane, 2-3-Dimethylbutane, n-Hexane, Hexafluorobenzene, MM, Pentafluorobenzene, n-Heptane, c-Hexane, MDM, n-Octane, D4, MD2M	$\eta_{is,turb} = 75\%$ $\eta_{wf,\ pump} = 60\%$	$\Delta T_{ml} = 30$ °C $\Delta T_{pp,rec} = 20$ °C $T_{cond} = 30$ °C $\Delta p_i = 0$	T_{eva}	Net power	Considerations on turbine design for power outputs 25–100 kW_{el}	–
Tchanche, Papadakis, et al. (2009) [8]	Solar: water @ 75–115 °C as HTF	2 kW_{el}	Sub-SA no-rec	RC318, R114, R113, R12, R123, R134a, R141b, R152a, R32, R407C, R500, Ethanol, Methanol, PropaneIsobutane, n-butane, n-pentane, Cyclohexane, NH_3, water,	$\eta_{is,turb} = 70\%$ $\eta_{wf,pump} = 80\%$ $\eta_{mec-el} = 63\%$	$\Delta T_{ap,PHE} = 15$ °C $\Delta T_{pp,PHE} = 6$ °C $T_{cond} = 35$ °C $\Delta p_i = 0$	–	–	Considerations on turbine outlet volume flow rate, volume flow ratio, and cycle pressures	$T_{HTF} = 90$ °C and $T_{eva} = 75$ °C: *n-butane*[c]*:* $\eta_{cycle} = 4.24\%$ $\eta_{II} = 24.8\%$
Dai et al. (2009) [4]	WHR: gas @145 °C	1100–1400 kW_{th} (15.95 kg/s)	Sub-SA rec/no-rec	NH_3, butane, isobutane, R11, R123, R141B, R236EA, R245CA, R113, water	$\eta_{is,turb} = 85\%$ $\eta_{wf,pump} = 60\%$	$\Delta T_{pp,PHE} = 8$ °C $\Delta T_{pp,rec} = 5$ °C $T_{cond} = 25$ °C $\Delta p_i = 0$	p_{eva} $T_{in,turb}$	Plant exergy efficiency	–	*R236ea:* $T_{eva} = 87.7$ °C $\eta_{cycle} = 11.53\%$ $\eta_{plant} = 7.88\%$[a] $\eta_{II} = 35.43\%$ *iso-butane:* $T_{eva} = 87.1$ °C $\eta_{cycle} = 11.52\%$ $\eta_{plant} = 7.79\%$[a] $\eta_{II} = 35.05\%$
Schuster et al. (2010) [26]	Generic source@ 210 °C	-	Sub-SA/Sup rec/no-rec	water, R134a, R227ea, R152a, RC318, R236fa, R245fa, isobutene, isopentane, isohexane, cyclohexane, R365mfc	$\eta_{is,turb} = 80\%$ $\eta_{wf,pump} = 85\%$	$p_{max} = 1.03^{*}p_{crit}$ (Sup cases) $\Delta T_{pp,PHE} = 10$ °C $\Delta T_{SH} = 2$ °C $\Delta T_{pp,rec} = 10$ °C $T_{cond} = 20$ °C $\Delta p_i = 0$	Sub: T_{eva} Sup: $T_{in,turb}$	Net plant efficiency	Heat exchangers area	*Sup:* *R365mfc & iso-pentane:* $T_{max} \approx 180$ °C $\eta_{plant} \approx 14\%$ *Sub:* *R245fa & iso-butene:* $T_{eva} \approx 140$ °C $\eta_{plant} \approx 13.2\%$
Lakew, Bolland (2010) [5]	WHR: air @ 80–200 °C	6–18 MW_{th} (100 kg/s)	Sub-SA no-rec	R134a, R123, R245fa, R227ea, n-pentane, Propane	$\eta_{is,turb} = 80\%$ $\eta_{wf,pump} = 80\%$ $\eta_{mec-el} = 90\%$	$\Delta T_{pp,PHE} = 10$ °C $\Delta T_{pp,cond} = 5$ °C $T_{cond} = 20$ °C $\Delta p_i = 0$	p_{eva}	Net power	Turbine (SP, single stage turbine), total HE area	$T_{ha} = 80–160$ °C: *R227ea* $T_{ha} = 200$ °C: *R245fa*
Quoilin, Orosz et al. (2011) [10]	Solar: with HTF @ ~150 °C	~60 kW_{th}	Sub-SA rec	n-pentane, SES36, R245fa, R134a	$\eta_{scroll-exp}$: calc $\eta_{wf,pump} = 70\%$ $\eta_{HTF,pump} = 70\%$	$\Delta T_{SH} = 10$ °C $\Delta T_{pp,PHE} = 8$ °C $\Delta T_{pp,rec} = 8$ °C $\Delta T_{pp,cond} = 8$ °C	T_{eva} ΔT_{HTF}	Net plant efficiency,	Scroll expander (given geometry), plate PHE area, recuperator area, condenser area	*SES36:* $T_{eva} = 169$ °C $\eta_{cycle} = 13.1\%$ $\eta_{plant} = 7.9\%$[b] *n-pentane:*

						$\Delta T_{sc,cond} = 5$ °C $\Delta p_{HEs} = 7.5$ kPa				$T_{eva} = 189$ °C $\eta_{cycle} = 11.9\%$ $\eta_{plant} = 7.0\%$[b]
Quoilin, Declaye et al. (2011) [6]	WHR: gas @ 180 °C with HTF.	92.9 kW_{th} (0.3 kg/s)	Sub-SA no-rec	R1234yf, R134a, R245fa, HFE7000, SES36, R123, n-butane, n-pentane	$\eta_{scroll-exp}$: calc $\eta_{wf,pump} = 60\%$ $\eta_{HTF,pump} = 60\%$ $\eta_{mec-el} = 70\%$	$\Delta T_{pp,PHE} = 10$ °C $\Delta T_{SH} = 5$ °C $\Delta T_{pp,cond} = 10$ °C $\Delta T_{sc,cond} = 5$ °C $T_{cw} = 15$ °C $m_{cw} = 0.5$ kg/s $\Delta p_{eva} = 10$ kPa $\Delta p_{cond} = 20$ kPa $\Delta T_{SH} = 5$ °C $\Delta T_{sc,cond} = 5$ °C $T_{cw} = 15$ °C $m_{cw} = 0.5$ kg/s	T_{eva} T_{eva} $\Delta T_{pp,PHE}$ $\Delta T_{pp,cond}$ Δp_{eva} Δp_{cond}	Net power Specific cost: €/kW	Scroll expander (given geometry), plate PHE area, condenser area	*R245fa:* $T_{eva} = 113.5$ °C $\eta_{cycle} = 7.78\%$ $\eta_{plant} = 5.13\%$ *R123:* $T_{eva} = 111.8$ °C $\eta_{cycle} = 8.41\%$ $\eta_{plant} = 5.00\%$ *n-butane:* $T_{eva} = 133.2$ °C $\Delta T_{pp,PHE} = 7.5$ °C $\eta_{plant} = 4.47\%$ Cs = 2136 €/kW *n-pentane:* $T_{eva} = 139.9$ °C $\Delta T_{pp,PHE} = 4.0$ °C $\eta_{plant} = 3.88\%$ Cs = 2505 €/kW
Shengjun et al. (2011) [14]	Geothermal brine @ 90 °C	~290 kW_{th} (1 kg/s)	Sub-SA/Sup no-rec	R123, R245ca, R245fa, R236ea, R236fa, R152a, R227ea, R134a, R143a, R218, R125, R41, R170, n-butane, Isobutane, CO_2	$\eta_{is,turb} = 80\%$ $\eta_{wf,pump} = 75\%$ $\eta_{mec-el} = 96\%$	$\Delta T_{pp,PHE} = 5$ °C $\Delta T_{pp,cond} = 5$ °C $T_{cw} = 20$ °C $\Delta p_i = 10$ kPa	Sub: T_{eva} p_{cond} Sup: $T_{in,turb}$ p_{max} p_{cond}	Specific heat exchange area (α): m^2/kW COE (only heat exchangers cost, function of operating pressure, considered)	Heat exchangers area	*R152a:* $T_{eva} = 74$ °C $T_{cond} = 27.9$ °C $\alpha = 1.64$ m^2/kW *R152a:* $T_{eva} = 60$ °C $T_{cond} = 27.9$ °C COE = 53 €/MWh
Zhang, Jiang (2012) [16]	Geothermal brine @ 100–200 °C	~310 kW_{th} 730 kW_{th} (1 kg/s)	Sub-SA/Sup no-rec	R134a, R245fa, isobutene, isopentane	$\eta_{is,turb} = 85\%$ $\eta_{wf,pump} = 85\%$	$\Delta T_{pp,PHE} = 4$ °C $\Delta T_{cond} = 35$ °C $T_{ca} = 26$ °C $\Delta p_i = 0$	T_{eva}	Plant exergy efficiency	–	$T_{geo} = 100$ °C: *R134a* ($T_{eva} = 68$ °C) $T_{geo} = 150$ °C: *R134a* (Sup) $T_{geo} = 200$ °C: *R245fa* (Sup)
Walraven et al. (2012) [17]	Geothermal brine @ 100–150 °C	~310 kWth 460 kWth (1 kg/s)	Sub/Sup rec/no-rec Bleed/no Bleed 1Pr. Lev. vs multi Pr..Lev.	R12, R22, R41, R32, R115, R124, R125, R134a, R142b, R152a, R218, R227ea, R236ea, R236fa, R245fa, R1234yf, R1234ze, RC318, C4F10, C5F12, CF3I, SF6, Ethane, Propane, iso-butane, Propylene, DME, CO_2, N_2O, others.	$\eta_{is,turb} = 85\%$ $\eta_{wf,pump} = 80\%$	$\Delta T_{pp,PHE} = 5$ °C $\Delta T_{cond} = 25$ °C $\Delta p_i = 0$	$T_{in,turb}$ p_{max}	Plant exergy efficiency	–	$T_{geo} = 125$ °C, no $T_{lim,geo}$: *R227ea* Sup, no-rec $\eta_{II} \sim 55\%$ $T_{geo} = 125$ °C, $T_{lim,geo} = 75$ °C: *R1234yf* Sup, rec $\eta_{II} \sim 41\%$

Note: Results of exergy analyses, where exergy losses due to incomplete cooling of the heat sources were not considered, are not included in Table 1.

[a] Heat available from WHR and geothermal brine calculated by considered cooling of the heat source to ambient temperature.

[b] Includes solar collector thermal efficiency.

[c] Optimal fluid considering constraints on component design.

- Possibility of selecting positive gauge condensing pressure, limiting the size of the low pressure components (condenser, turbine discharge and low pressure vapor piping) and avoiding air in-leakages.

For all these reasons, organic Rankine cycles are experiencing a great commercial success and an increased interest in the R&D activities for the optimization of new ORC cycles and the related components [2].

A number of scientific studies has been published relatively recently on the selection of working fluids and on the optimization of the corresponding cycle parameters for a number of applications, namely waste heat recovery [3–6], biomass combustion [7], solar heat [8–10], geothermal sources [11–17] and geothermal-solar hybrid concepts [18]. Advanced cycle configurations, such as supercritical cycles [14,16,17,19–21] and multi-level cycles [17,22], the use of mixtures [23,24] and predictive theoretical methods to define the optimal working fluids [25] are also being explored.

From the selection of works reported in Table 1, it is evident that dedicated optimization analyses are required for each specific application, due to the wide range of temperatures (~70–350 °C) and sizes (from few kW_{el} to tens of MW_{el}) of the potential heat source. In addition, the increasing restrictions in the use of fluids with high GWP and ODP and safety issues (flammability and toxicity) make it important to investigate the performance of new environmental friendly and low risk fluids. All these factors justify the abundant literature recently produced on this topic.

The aim of this work is to present thermodynamic and techno-economic assessment and optimization of ORCs based on different cycle configurations (subcritical/supercritical, saturated/superheated, regenerative/non regenerative), operating with a variety of working fluids, for the exploitation of low-medium enthalpy geothermal fields (120–180 °C) in the 2–15 MW_{el} power output range. The results of the thermodynamic analysis are firstly presented, discussing some general rules relating the critical temperature of the optimal fluid to the heat source temperature. The results of the techno-economic study are then discussed in Part B of the paper.

2. Model description

A Matlab® [27] code was implemented in order to perform both thermodynamic and techno-economic optimizations of binary systems based on ORC technology. Single pressure level cycles in saturated/superheated, regenerative/non-regenerative, subcritical/supercritical configurations are considered as shown in Table 2.

The choice of the optimal cycle configuration is strictly related to the considered working fluid, since only a correct selection of both fluid and cycle configuration allows achieving the best performance. Currently, in almost all the commercial applications a limited number of fluids is used: refrigerants and short chained alkanes are typically adopted for low temperature applications. On the contrary, a large number of fluids is considered in this study, in order to cover a wide range of critical temperatures and pressures, molecular weights and complexity. The developed code is integrated with the Refprop® database [28] that uses accurate equations of state to provide the thermodynamic properties of a large variety of fluids. The list of the 54 pure fluids selected in this study is reported in Table 3. Refrigerant mixtures are not considered here, even if potential advantages can be achievable thanks to temperature glide along evaporation and condensation.

The wide variety of fluids considered allows investigating different cycle configurations with the possibility to select the combination of working fluid and design parameters that is able to maximize plant performances. Besides thermodynamic results that are treated in this study, many other aspects have to be considered in fluid selection. In particular thermal stability is a crucial parameter in order to prevent chemical decomposition during plant operation, to avoid formation of sludge which can damage turbomachines and heat exchangers surfaces and to limit cost related to fluid substitution, etc. In this work maximum attainable temperatures are below the stability limit of almost all the selected fluids and so no difficulties rise in most of the investigated cases. Only seven of the selected fluids have a thermal stability limit lower than 200 °C. For these fluids the maximum temperature is selected according to the validity limit of the equation of state used in Refprop®. Other technical aspects to consider when selecting a working fluid are related to safety issues such as toxicity and flammability. In particular, the use of alkanes and hydrocarbons, which are flammables, introduces hazards in plant operation and requires additional safety measures. Similarly ammonia, which is highly toxic, needs proper safety measures. On the contrary most of all HFCs, FCs and siloxanes are totally safe, being non-toxic and flammable only under extreme ignition conditions.

From an environmental point of view two indexes are usually adopted, namely GWP and ODP which measure the impact on greenhouse effect and ozone depletion respectively. For these reasons, hydrochlorocarbons and hydrochlorofluorocarbons, even if they are available in the Refprop® database, are not considered in this study, being banned in Europe due to their high ODP index.

Fig. 1 presents the basic layout of a regenerative, subcritical superheated cycle, in order to define the notation which will be used in following discussions. This cycle is composed by a series of heat exchangers (economizer, evaporator, superheater), a turbine, a regenerator, a condenser and a pump. the regenerator is used to preheat the condensate at the pump outlet by recovering part of the heat released at the turbine outlet during fluid desuperheating. For non-regenerative cycles, points 10 and 3 simply collapse in 9 and 2 respectively, while in saturated cycles point 7 coincides to 6 and in supercritical configuration points 4, 5 and 6 merge to 7.

The plant performance can be evaluated once defined the value of all the model variables: some of these, labeled as fixed variables, are assumed prior to calculation and kept constant in the thermodynamic optimization procedure, independently on fluid and cycle configuration. The others, labeled as design variables, are set

Table 2
Investigated cycle configurations.

Subcritical	Superheated	Regenerative
		Non-regenerative
	Saturated	Regenerative
		Non-regenerative
Supercritical		Regenerative
		Non-regenerative

Table 3
Investigated fluids.

12	Alkanes	Propane, Isobutane, Butane, Neopentane, Isopentane, Pentane, Isohexane, Hexane, Heptane, Octane, Nonane, Decane
16	Other hydrocarbons	Cyclopropane, Cyclopentane, Cyclohexane, Methylcyclohexane, Propylcyclohexane, Isobutene, 1-Butene, Trans-Butene, Cis-Butene, Benzene, Propyne, Methanol, Ethanol, Toluene, Acetone, Dimethylether
13	HFC	R125, R143a, R32, R1234yf, R134a, R227ea, R161, R1234ze, R152a, R236fa, R236ea, R245fa, R365mfc
3	FC	R218, Perfluorobutane (C_4F_{10}), RC318
8	Siloxanes	MM, Mdm, Md2m, Md3m, Md4m, D4, D5, D6
2	Other non-organic fluids	Ammonia, water

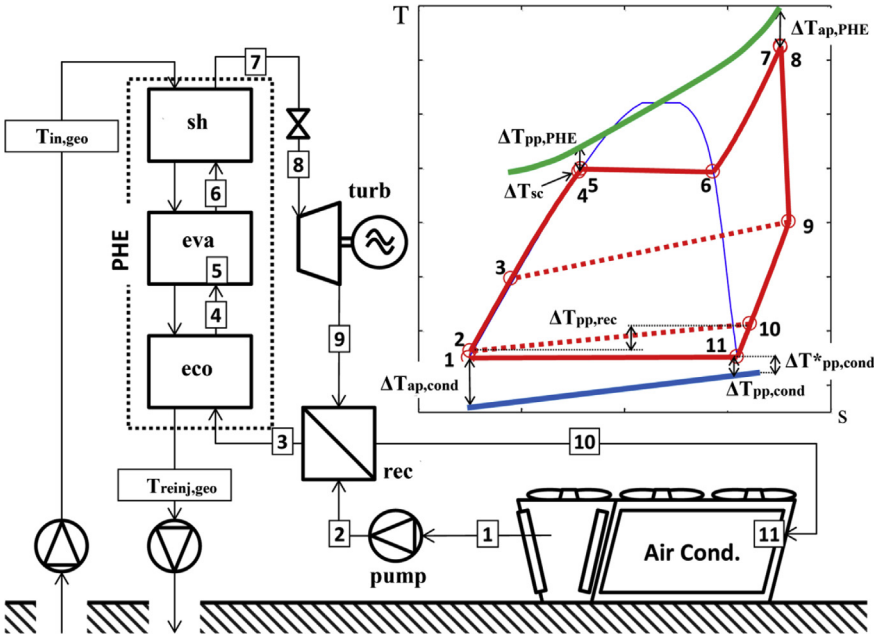

Fig. 1. *T–s* diagram, plant layout and notation adopted to define thermodynamic points.

up by the optimization routine. All the variables are reported in Table 4.

Relative pressure drops for vapor streams are referred to the component inlet pressure, while absolute pressure drops are assumed for liquid streams. For the two-phase heat exchangers saturated temperature drops rather than pressure drops are defined.

A shell and tube PHE (primary heat exchanger) is considered, arranged either in once-through configuration in supercritical cycles or as kettle reboiler evaporator in subcritical cycles. In this last case, a sub cooling temperature difference is assumed as fixed percentage of the temperature increase in the economizer, but constrained to at least 1 °C as reported in Table 4.

Turbine isentropic efficiency is assumed constant throughout the thermodynamic optimization and performance dependence on fluid properties and operating conditions will be introduced in the Part B of the present paper as well the possibility to adopt a gearbox in order to decouple the turbine and the generator rotational speeds.

On the basis of manufacturers of air cooled condensers experience [29], the simplified empirical relations reported in Fig. 2 have been derived from numerical and experimental data to calculate the heat exchange area and the fan power consumption, which gives a relevant contribution to the auxiliary power consumption. Correlations in Fig. 2 are obtained by considering the organic fluid at inlet at saturated vapor conditions.

Finally, in order to avoid the formation of droplets within the turbine, the expansion is always constrained in the superheated vapor region. For fluids with overhanging saturation line, vapor quality is computed along all the expansion by dividing it into several steps, while in the case of bell shaped saturation line a check on exhaust quality is sufficient.

Plant performance is also strongly influenced by the hypothesis related to geothermal brine properties and ambient conditions. If not otherwise stated, ambient temperature is set equal to 15 °C while hypotheses related to brine mass flow, inlet temperature and reinjection temperature limit will be defined for each investigated case. Heat capacities of ambient air and geothermal brine are kept constant neglecting the effects related to temperature, incondensable gases and dissolved salts in the geothermal water, which is hence considered pure and always at liquid state.

Once fixed variables are assigned, all the thermodynamic points of the ORC cycle can be sequentially calculated with the definition of six independent design parameters:

- Turbine inlet pressure ($p_{in,turb}$): it is the pressure in point 7 just ahead of turbine admission valve; this parameter strongly affects the thermodynamic efficiency, the working fluid mass flow

Table 4
Assumed fixed and variable parameters adopted for the thermodynamic analysis.

Objective function	η_{II}
Design variables	
$p_{in,turb}$	Optimized
$\Delta T_{ap,PHE}$	Optimized
$\Delta T_{pp,PHE}$	3 °C
$\Delta T_{pp,rec}$	5 °C
$\Delta T_{ap,cond}$	15 °C
$\Delta T^{*}_{pp,cond}$	0.5 °C
Temperature and pressure drops	
ΔT_{cond}	0.3 °C
ΔT_{eva}	1 °C
Δp_{des}	1%
Δp_{SHE}	5%
Δp_{sh}	2%
Δp_{val}	1%
$\Delta p_{rec,HS}$	2%
Δp_{eco}	50 kPa
$\Delta p_{rec,CS}$	50 kPa
Heat losses from heat exchangers	
Q_{loss}	1%
Other assumptions	
$\eta_{is,turb}$	85%
$\eta_{wf,pump}$	70%
$\eta_{mec\text{-}ele,pump}$	95%
$\eta_{mec\text{-}ele,turb}$	95%
$\eta_{gear\ box}$	97%
ΔT_{sc}	max(1 °C, 0.05(T_5−T_3))
Constrain	
No droplets along expansion	

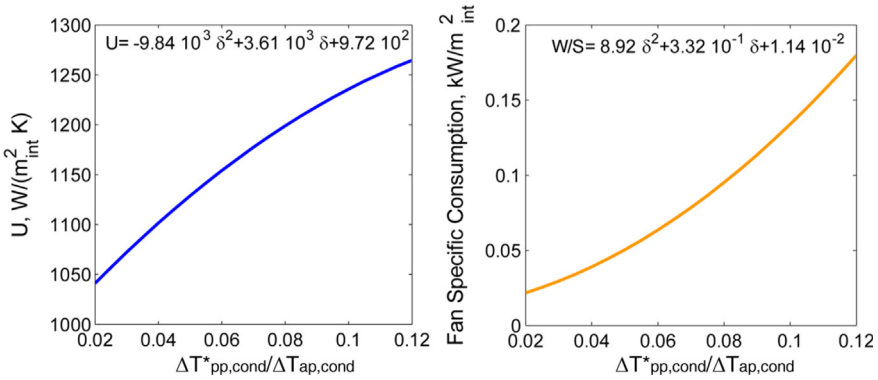

Fig. 2. Correlation for U and W/S for the air condenser unit for ambient temperatures between 15 and 25 °C. The range of fan velocity investigated corresponds to frontal air velocities between 1.0 and 2.5 m/s. Organic fluid at inlet is assumed at saturated vapor conditions. The effect of de-superheating in the range experienced in this work has been tested on some fluids considered in this work, leading to maximum errors of the thermal power of 2% with respect to a condition of saturated vapor condensation.

and PHE heat transfer area. In case of subcritical cycles, evaporation temperature and pressure directly depend on this parameter.

- Approach point temperature difference in PHE ($\Delta T_{ap,PHE}$): it is the difference between the inlet temperature of the geothermal brine and turbine inlet temperature. In case of subcritical cycles, $\Delta T_{ap,PHE}$ is constrained to not exceed the maximum value corresponding to the saturated cycle condition.
- Approach point temperature difference at the condenser ($\Delta T_{ap,cond}$): this parameter defines the temperature of the saturated liquid discharged from the condenser. Reducing this parameter leads to an increase in the gross power output but also to a rise of the ORC pump and the condenser fans consumption. In addition, also the condenser surface increases leading to a higher power block cost.
- Pinch point temperature difference in the recuperator ($\Delta T_{pp,rec}$): it is the temperature difference between points 2 and 10. This parameter influences the regenerator effectiveness. Its optimization is important in presence of a limit on the geothermal brine reinjection temperature because a proper recuperator design allows obtaining the best compromise between cycle efficiency and exploitation of the geothermal heat available.
- The pinch point temperature difference in PHE $\Delta T_{pp,PHE}$ (or the equivalently reinjection temperature of the geothermal brine $T_{reinj,geo}$). By reducing the reinjection temperature and the pinch point ΔT, on one side the heat recovery and the overall plant efficiency increase, on the other side the PHE area and cost also increase.
- The modified pinch point temperature difference in the air condenser ($\Delta T^{*}_{pp,cond}$). Defined as the temperature difference between the saturated vapor in the condenser and the air at condenser outlet, as shown in Fig. 1. By reducing this parameter, a lower air flow rate is used with reduced fan consumption, but a higher heat transfer area is required, leading to a higher condenser cost.

Once all thermodynamic properties and mass flows are determined, it is possible to calculate the UA parameters which give a reasonable indication of the heat exchangers dimension. In particular, UA is computed by dividing each heat exchanger, with the exception of evaporator and condenser, into several sections to account for specific heat variation vs. temperature. The total UA parameter is then calculated according to the following formula:

$$UA_{HE} = \sum_{i} \frac{Q_i}{\Delta T_{ml,i}} \tag{1}$$

where log mean temperature difference in each section is computed considering a constant specific heat.

The net plant power is thus computed as the difference between the gross turbine generator power output and the consumption of the pump and of the condenser fans. Finally, the following performance indexes can be calculated:

$$\eta_{cycle} = \frac{W_{net}}{Q_{in}} \tag{2}$$

$$\eta_{rec} = \frac{Q_{in}}{Q_{in,\,max}} \tag{3}$$

$$\eta_{plant} = \eta_{cycle}\eta_{rec} = \frac{W_{net}}{Q_{in,\,max}} \tag{4}$$

$$\eta_{II} = \frac{\eta_{plant}}{\eta_{lor}} \tag{5}$$

$$\eta_{lor} = 1 - \frac{T_{amb}}{\ln\left(\frac{T_{in,geo}-T_{lim,geo}}{T_{in,geo}/T_{lim,geo}}\right)} \tag{6}$$

where $T_{lim,geo}$ is the minimum reinjection temperature for the geothermal brine in order to avoid salt precipitation on heat exchangers surfaces and $Q_{in,max}$ is the maximum thermal power that can be recovered by cooling the geothermal brine down to $T_{lim,geo}$ (or ambient temperature, when no reinjection temperature limit is considered). Q_{in} is the thermal power released by the geothermal brine when cooled in the ORC heat exchangers and hence the thermal power received by the ORC divided by the thermal efficiency of the heat exchangers.

It is important to highlight here that the cycle efficiency is just a parameter useful for the interpretation of the results obtained, but cannot be used as optimization parameter in geothermal plants. As a matter of fact, increasing the cycle efficiency often leads to a reduction of the heat recovery rate. For this reason, in our analysis we will always refer to net power, plant efficiency or second law efficiency as term of comparison among the different solutions. It is important to note that Lorentz efficiency refers to an ideal trapezoidal cycle if a limit in reinjection temperature is considered or to a trilateral cycle otherwise [30]. This definition entails that the higher the geothermal brine minimum reinjection temperature, the higher η_{lor}, because of the higher heat introduction mean logarithmic temperature.

All the assumptions aforementioned are reported in Table 4.

3. Thermodynamic optimization

The first step of our study is an extensive thermodynamic optimization of binary geothermal power plants with the target to define the best combination of fluid and cycle configuration for different geothermal brine temperatures. The objective function is plant efficiency (or equivalently the net power output or second law efficiency η_{II}), to be maximized for a given geothermal source.

The thermodynamic optimization is conducted by assigning constant reasonable values to four of the six design parameters, whose optimal values are strictly related to economic considerations, while optimizing the two remaining ones. As shown in Table 4, the two optimization variables are the turbine inlet pressure and the approach point temperature difference in the PHE.

Different optimization algorithms have been tested to identify the most reliable one in terms of solution accuracy and computational time. Optimization is performed with the Matlab *fmincon* function using an Active-set algorithm. Tolerances for objective values and optimization variables are considered equal to 1e-5 (relative difference between two solutions).

3.1. Thermodynamic optimization with 150 °C geothermal brine

In order to outlight the influence of the two optimization parameters on the final thermodynamic performance, let's first discuss the results for two different cases corresponding to a supercritical regenerative cycle with R134a and a R245fa subcritical regenerative cycle presented in Figs. 3–5. Geothermal brine temperature is fixed equal to 150 °C and the rejection temperature is limited to 70 °C. Different combinations of $p_{in,turb}$ and $\Delta T_{ap,PHE}$ are investigated. From the contour diagrams in Fig. 3 referred to R134a cycles, it is possible to note that the optimal results are obtained for

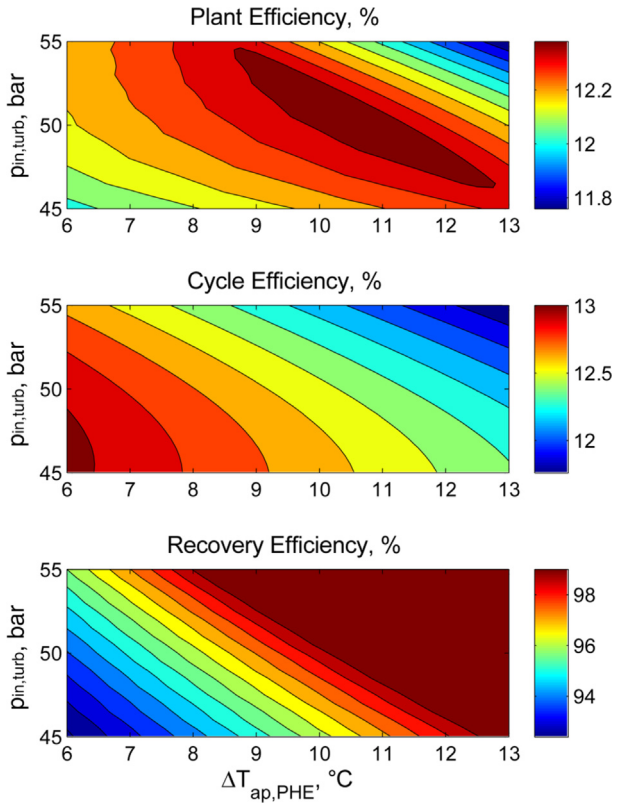

Fig. 3. Thermodynamic optimization results for R134a supercritical cycle.

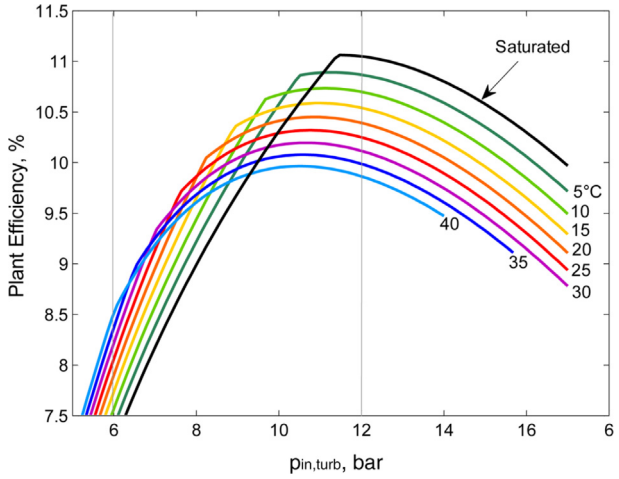

Fig. 4. Optimization results for a R245fa subcritical cycle with regeneration, with different levels of superheating.

the cycles with the best compromise between cycle and recovery efficiency. For a given $p_{in,turb}$, reducing $\Delta T_{ap,PHE}$ (i.e. increasing the turbine inlet temperature) allows reaching higher values of the cycle efficiency, but above a certain limit yields a lower heat recovery from geothermal brine. Optimum value of $\Delta T_{ap,PHE}$ is higher than the lower bound and, for a given turbine inlet pressure, it is near the maximum value for which a heat recovery efficiency of 100% is obtained.

The results for R245fa are presented in Fig. 4 where parametric curves for different values of ΔT_{sh} are reported and compared with the values which can be obtained for a saturated cycle. By observing the trend of one of the reported curves, it is possible to note that at low evaporation pressures, geothermal brine is totally exploited and an evaporation temperature increase is convenient because it entails higher cycle efficiency. This occurs up to a certain pressure, over which plant efficiency suddenly starts decreasing, or for low ΔT_{sh} values a discontinuity can be highlight. Here, the minimum pinch point temperature difference in PHE becomes the active constraint and geothermal brine reinjection temperature is higher than the limit entailing a recovery efficiency drop with detrimental effects on cycle performance. As widely observed in the literature for organic fluids, it is evident that saturated cycle is the optimal solution and the superheating is detrimental for thermodynamic performance.

The situation is illustrated In Fig. 5, where the influence of superheating is analyzed for two turbine inlet pressures: while at low pressure increasing superheating is beneficial, mostly due to lower irreversibilities in the heat introduction in the evaporation phase and in the economizer, for higher pressure the reduced exergy losses in heat exchangers are overcompensated by the higher residual exergy in the brine discharged. This analysis, repeated for different fluids with high critical temperature and overhanging saturation line, suggests that the best performance is generally reached for saturated cycle with the higher value of evaporation pressure consistent with the rejection temperature constraint, as already highlighted in other studies [4,13].

Optimal combination of working fluid and cycle configuration changes, when different assumptions for geothermal brine and ambient temperatures are made. As a matter of fact, for a given inlet brine temperature, the reinjection temperature limit and the ambient temperature affect the final optimal solution. The results of the sensitivity analysis performed on these parameters are shown in Fig. 6.

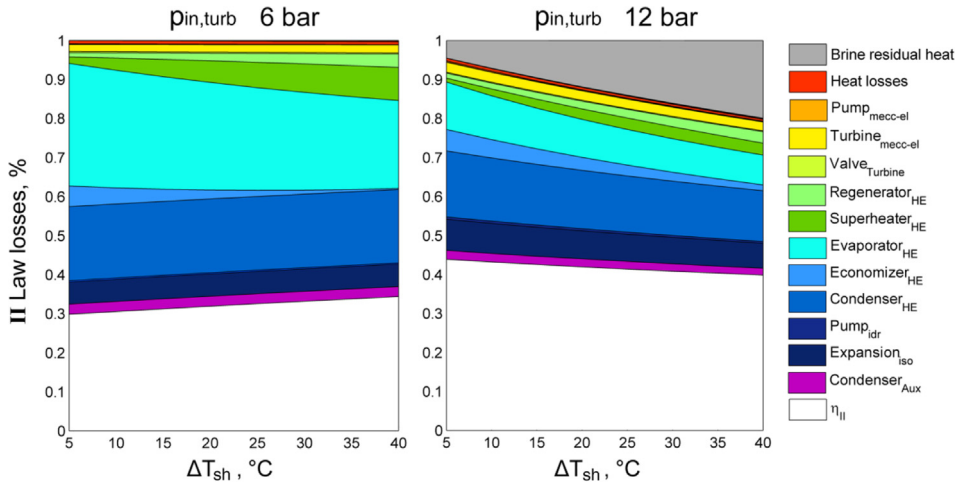

Fig. 5. Second law analysis for R245fa subcritical cycle with regeneration for two evaporation pressures and different approach point temperature difference at superheating.

In Fig. 6a it is assumed there is no limit in cooling down of the geothermal brine, while in Fig. 6b it is set a limit of 70 °C. Finally Fig. 6c outlines the effect of a higher ambient temperature.

Results are displayed for all the considered fluids and all the investigated cycle configurations, which are marked with different colors. The three top ranked cycles for each case are also reported in Table 5.

In all the considered cases, the best plant efficiencies occur for the supercritical cycles adopting fluids with critical temperature slightly lower than the geothermal brine one. As a matter of fact, in these cases it is possible to strongly reduce the ΔT_{ml} in the PHE, thus limiting the exergy losses during heat transfer. For fluids with higher critical temperatures, it is not possible to obtain supercritical cycles and saturated cycles are always the best solution as already pointed out. It is also interesting to note that for values of $T_{crit}/T_{in,geo}$ higher than 0.95, all the optimal solutions have roughly the same efficiency. This result can be explained by considering that all these cycles are saturated cycles with a similar evaporation temperature and hence a similar average temperature of heat input.

As far as the regenerator is concerned, regenerative cycles are suggested for cases (b) and (c) because of the limitation on the reinjection temperature, while in case (a) regenerator is not profitable because it limits the exploitation of geothermal brine. However, the adoption of a regenerative cycle should not be excluded a priori even for this case, neither from a thermodynamic nor from an economic point of view. As a matter of fact, the

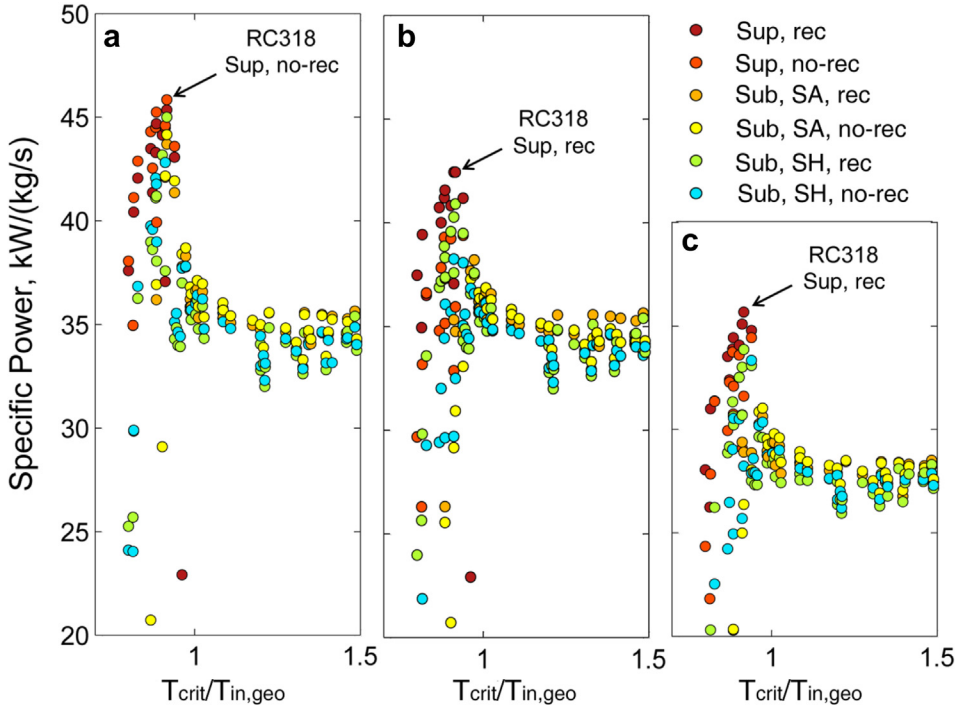

Fig. 6. Comparison among three different cases for a 150 °C geothermal brine: (a) $T_{amb} = 15$ °C, $T_{lim,geo} = 15$ °C, (b) $T_{amb} = 15$ °C, $T_{lim,geo} = 70$ °C and (c) $T_{amb} = 25$ °C, $T_{lim,geo} = 70$ °C. Each dot refers to a different cycle configuration.

Table 5
Results of the thermodynamic optimization for 150 °C geothermal brine temperature and different ambient and brine reinjection temperatures.

	T_{amb} °C	$T_{lim,geo}$ °C	Ranking	Fluid	Plant configuration	$T_{crit}/T_{in,geo}$	Specific power kW/(kg/s)	η_{cycle} %	η_{rec} %	η_{plant} %	η_{II} %
a)	15	15	1°	RC318	SUP, no-rec	0.918	45.82	10.20	80.33	8.20	45.54
			2°	R227ea		0.886	45.21	9.84	82.13	8.08	44.94
			3°	C_4F_{10}		0.913	44.57	9.47	84.14	7.97	44.30
b)	15	70	1°	RC318	SUP, rec	0.918	42.41	12.83	99.65	12.79	52.17
			2°	C_4F_{10}		0.913	42.41	12.79	100.0	12.79	52.17
			3°	R227ea		0.886	41.54	12.53	100.0	12.53	51.10
c)	25	70	1°	RC318	SUP, rec	0.918	35.64	10.76	99.80	10.75	49.09
			2°	C_4F_{10}		0.913	35.06	10.67	99.15	10.58	48.29
			3°	R227ea		0.886	34.40	10.44	99.38	10.37	47.38

regenerator entails higher cycle efficiency and reduces the heat to be rejected by the condenser, thus reducing its cost and the parasitic consumption of the fans.

In all the cases, RC318, C_4F_{10} and R227ea appear as the best fluids from the thermodynamic point of view. This result is not surprising because these fluids have a similar number of carbon atoms (four carbon atoms for RC318 and C_4F_{10} and three for R227ea) and differ in the number of fluorine atoms and the chain arrangement. These analogies entail a similar shape of the saturation line and an almost equal critical temperature and therefore very similar results in the three investigated cases.

3.2. Thermodynamic optimization for different geothermal brine temperatures

Thermodynamic optimization is carried out for all the fluids reported in Table 3, considering five geothermal brine temperatures between 120 °C and 180 °C, representative of different geothermal fields. As on the previous case the analysis is repeated with two different assumptions for the rejection temperature, namely: no reinjection temperature limit and minimum reinjection temperature of 70 °C.

A comparison among the five investigated cases with no reinjection temperature limit is reported in Fig. 7, where each point represents the best cycle configuration for a given working fluid. Firstly, it is possible to note that for the different geothermal brines considered, the same trend is obtained with the $T_{crit}/T_{in,geo}$ ratio. This is quite interesting and suggests the possibility to define some

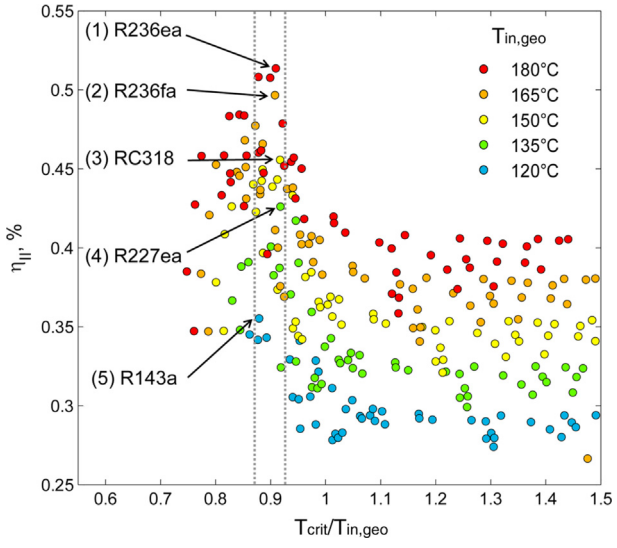

Fig. 7. Second law efficiency for five geothermal brine temperatures between 120 and 180 °C.

global rules in the simultaneous selection of cycle configuration and working fluid. For all the considered cases, the optimal fluid has a critical temperature which lies in a very small range between 0.88 and 0.92 of the geothermal brine temperature. In addition, as shown in Fig. 8a, all the selected cycle configurations are supercritical cycles with reduced pressures between 1.1 and 1.6. Coherently with the assumption of no reinjection temperature limit, regeneration is never adopted in the optimal cycle configurations.

From a thermodynamic point of view it is hence possible to conclude that for a given geothermal source a pre-selection can be made among a small number of working fluids which allows, in supercritical configuration, to achieve the highest performances. However, as shown in Fig. 8b, the adoption of supercritical cycles leads to higher values of $\Sigma UA/W_{net}$ compared to subcritical saturated ones. Therefore, higher heat exchange area and cost can be expected for optimized supercritical cycles, highlighting the importance of an economic analysis to define the optimal combination of fluid and plant configuration, as discussed in Part B of the paper.

As already highlighted, when a reinjection temperature limit is considered, the optimal cycle configuration requires the adoption of a regenerator. As shown in Table 6, where the optimal cycles for different geothermal brine conditions are reported, for medium/high temperature of geothermal brine (150–180 °C), the optimal fluid is the same as the optimal one selected for the unconstrained reinjection temperature case. The supercritical cycle still remains the optimal solution, but the sharp peak shown in Figs. 7 and 8 is less pronounced, showing small advantages over subcritical cycles. In addition, regeneration gives a significant contribution to achieve the best performance. For the lowest geothermal brine temperature considered (120 °C), the optimal fluid is C_4F_{10}, which has a critical temperature higher than R143a and the optimal configuration is a regenerative saturated cycle. This can be explained considering the low temperature difference available for geothermal brine cooling, corresponding to the exploitation of a heat source at almost constant temperature, which leads to no advantage in the adoption of a supercritical "nearly triangular" cycle.

Finally, some considerations on the influence of molecular complexity on the optimal fluid selection can be made. Complex fluids have similar specific heat in vapor and liquid phase, therefore their Andrews saturation line becomes overhanging. This characteristic allows designing PHE with very small ΔT_{ml} taking advantage from the relatively small heat capacity variation below and over the critical point.

This last point can be explained by considering two fluids with a similar critical temperature but different molecular complexity. The selected fluids are C_4F_{10} and R152a, whose backbone chains have four and two carbon atoms respectively. C_4F_{10} is a cycloalkane fully substituted by fluorine atoms, while R152a chemical formula is $F_2HC{-}CH_3$. Results obtained for the thermodynamic optimization are reported in Table 7, while $T{-}s$ and $T{-}Q$ diagrams are shown in Fig. 9. Using a more complex fluid like C_4F_{10} gives the possibility to

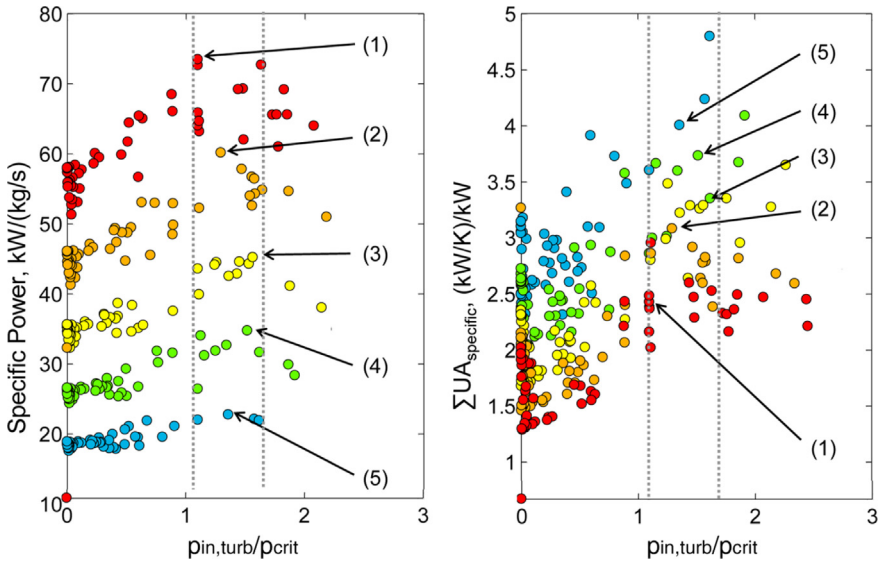

Fig. 8. Specific power and specific UA for five geothermal brine temperatures between 120 and 180 °C. Optimal fluid for each geothermal brine temperature is labeled with a number with reference to Fig. 7.

Table 6
Best fluid and cycle configuration obtained for three geothermal brine temperatures with two different assumptions on reinjection temperature.

$T_{in,\ geo}$		$T_{lim,geo}$ = 15 °C	$T_{lim,geo}$ = 70 °C
180	Optimal fluid	R236ea (Sup, no-rec)	R236ea (Sup, rec)
	$T_{crit}/T_{in,geo}$	0.912	0.912
	η_{cycle}, %	14.42	15.28
	η_{rec}, %	74.54	100.0
	η_{plant}, %	10.75	15.28
	Specific power kW/(kg/s)	73.48	69.65
150	Optimal fluid	RC318 (Sup, no-rec)	RC318 (Sup, rec)
	$T_{crit}/T_{in,geo}$	0.918	0.918
	η_{cycle}, %	10.20	12.83
	η_{rec}, %	80.33	99.65
	η_{plant}, %	8.20	12.79
	Specific power kW/(kg/s)	45.82	42.41
120	Optimal fluid	R143a (Sup, no-rec)	C_4F_{10} (Sub, SA, rec)
	$T_{crit}/T_{in,geo}$	0.880	0.983
	η_{cycle}, %	7.73	9.65
	η_{rec}, %	67.66	99.70
	η_{plant}, %	5.23	9.62
	Specific power kW/(kg/s)	22.75	19.93

Table 7
Thermodynamic results and second law analysis comparison between fluids with the same critical temperature but different molecular complexity, for $T_{in,\ Geo}$ = 150 °C and $T_{limit,\ Geo}$ = 70 °C.

			C_4F_{10}	R152a
T_{crit}		°C	113.28	113.26
Specific power		$kW_{el}/(kg/s)$	42.41	38.53
η_{cycle}		%	12.79	12.17
η_{rec}		%	100.0	95.46
η_{plant}		%	12.79	11.62
$\sum UA_{specific}$		$(kW_{th}/K)/kW_{el}$	3.205	2.589
$\Delta T_{ml,PHE}$		K	4.49	8.87
η_{II}		%	52.17	46.93
$\Delta\eta_{II}$	Expansion	%	10.50	10.32
	Pump	%	3.63	2.50
	PHE	%	4.63	12.94
	Condenser heat transfer	%	18.14	17.15
	Regenerator heat transfer	%	3.91	–
	Turbomachinery $_{mecc-el}$	%	4.41	3.80
	Heat exchangers heat losses	%	0.17	0.97
	Condenser Aux	%	2.45	2.34
	Brine residual heat	%	0.00	3.05

reduce heat transfer irreversibilities in PHE while the adoption of a regenerator allows increasing the cycle thermodynamic efficiency without penalizing the heat recovery efficiency. On the other hand, the use of C_4F_{10} demands for larger PHE heat transfer area and cost, highlighting once again the importance of economic analyses in a comprehensive optimization procedure. In Table 7, results of the second law analysis are also reported. In both cases, losses related to heat discharged by the condenser have the greatest impact, highlighting the importance of irreversibilities in heat rejection for cycles with a limited efficiency. As expected, the main difference is associated to the PHE, with a strong exergy losses reduction by moving towards higher complexity fluids. Finally, the effect of the recovery efficiency is reflected in the brine residual heat loss, which contributes reducing the efficiency of R152a, even considering the additional losses in the regenerator present only for C_4F_{10}.

4. Conclusions

This work presents the results of thermodynamic optimization applied to a large number of working fluids and to various cycle configurations for the exploitation of medium-low temperature geothermal brines. In this first part the optimization is carried out

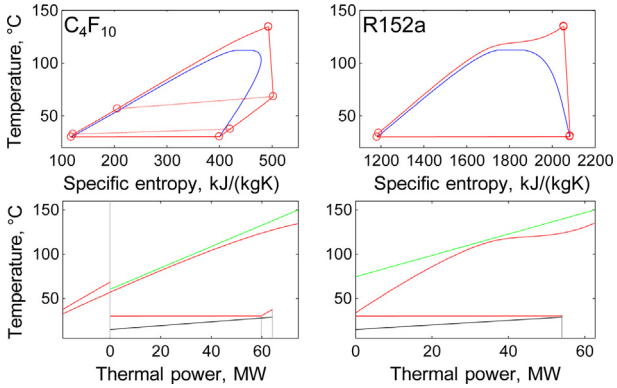

Fig. 9. *T–s* and *T–Q* diagrams for fluids with the same critical temperature but different molecular complexity.

by varying two parameters, $p_{in,turb}$ and $\Delta T_{ap,PHE}$, while all the other variables (pressure drops, turbomachinery efficiencies, temperature differences in regenerator and condenser units) are fixed on the basis of data from literature, real power plants data sheets and preliminary design considerations.

By analyzing the results obtained with different geothermal brine temperatures, some general trends can be highlighted and the following consideration can be outlined:

- Optimal plant efficiencies are obtained for fluids with a $T_{crit}/T_{in,geo}$ parameter between 0.88 and 0.92 and a supercritical cycle with a reduced pressure between 1.1 and 1.6. Only in case of small maximum geothermal brine ΔTs (in contemporary presence of a reinjection temperature limit and a low brine temperature), subcritical cycles show better performance.
- When subcritical cycles are considered, superheating is not profitable and optimal cycles have a saturated cycle configuration.
- If no reinjection temperature limit is considered, the optimal cycle configuration is a non-recuperative one, because of the convenience of a full exploitation of the available geothermal heat. Otherwise, if a constraint on reinjection temperature is assumed, regeneration is profitable and allows increasing cycle efficiency without penalizing the recovery rate.
- Adopting a supercritical cycle allows to achieve high performances but increases total surface area, which shows the importance of considering also economic aspects in a comprehensive optimization procedure.
- Among fluids with a similar critical temperature, fluids with high molecular complexity are preferable because of the possibility to reduce the average temperature differences in the primary heat exchanger, hence limiting the exergy losses.

Nomenclature

Acronyms

COE	cost of electricity €/MWh
FC	fluoro carbons
GWP	global warming potential index
HFC	hydro-fluoro carbons
HTF	heat transfer fluid
ODP	ozone depletion potential index
ORC	organic Rankine cycles
PHE	primary heat exchanger
R&D	research and development
WHR	waste heat recovery

Notation

A	heat exchanger surface m^2
p	pressure bar
Q	thermal power kW
rec/no-rec	recuperative/non recuperative cycle configuration
SA	saturated or slightly superheated cycle
SH	superheated cycle
Sub	subcritical cycle
Sup	supercritical cycle
T	temperature °C
u	fluid velocity in heat exchangers m/s
U	global heat transfer coefficient kW/(m^2K)
W	power kW
α	specific heat exchange area m^2/kW
Δp	pressure difference bar
ΔT	temperature difference °C
η	efficiency %

Subscripts

amb	ambient conditions
ap	approach point
ca	cooling air
cond	condensation (condition) or condenser (plant component)
crit	critical condition
CS	HE cold side
cw	cooling water
des	desuperheating section of condenser (plant component)
eco	economizer (plant component)
el	electrical
eva	evaporation (conditions) or evaporator (plant component)
geo	geothermal brine
ha	hot air from WHR
HS	HE Hot Side
II	second law
in	inlet condition
is	isentropic process
lim	limit in reinjection condition
lor	lorentz (efficiency)
loss	dispersion to the environment
mec	mechanical
ml	mean logarithmic
PHE	primary heat exchanger
pp	pinch point
Pr. Lev	pressure level (for subcritical cycles)
rec	recovery (efficiency) or regenerator (plant component)
reinj	reinjection condition
sc	sub cooling
scroll-exp	scroll expander
sh	superheater (plant component)
SHE	supercritical PHE turbturbine (plant component)
val	valve at turbine inlet (plant component)
wf	working fluid

References

[1] Macchi E. Design criteria for turbines operating with fluids having a low speed of soundIn Lecture series 100, Brussels. Von Karman Institute for Fluid Dynamics; 1977.

[2] Chen H, Goswami DT, Stefanakos EK. A review of thermodynamic cycles and working fluids for the conversion of low-grade heat. Renew Sustain Energy Rev 2010;14:3059–67.

[3] Invernizzi C, Iora P, Silva P. Bottoming micro-Rankine cycles for micro-gas turbines. Appl Therm Eng 2007;27(1):100–10.

[4] Dai Y, Wang J, Gao L. Parametric optimization and comparative study of organic rankine cycle (ORC) for low grade waste heat recovery. Energy Convers Manag 2009;50:576–82.

[5] Lakew A, Bolland O. Working fluids for low-temperature heat source. Appl Therm Eng 2010;30(10):1262–8.

[6] Quoilin S, Declaye S, Tchanche BF, Lemort V. Thermo-economic optimization of waste heat recovery organic Rankine cycles. Appl Therm Eng 2011;31:2885–93.

[7] Drescher U, Brüggemann D. Fluid selection for the organic Rankine cycle (ORC) in biomass power and heat plants. Appl Therm Eng 2007;27:223–8.

[8] Tchanche BF, Lambrinos G, Frangoudakis A, Papadakis G. Low-grade heat conversion into power using organic rankine cycles – a review of various applications. Renew Sustain Energy Rev 2009;15(8):3963–79.

[9] Rayegan R, Tao YX. A procedure to select working fluids for solar organic Rankine cycles (ORCs). Renew Energy 2011;36(2):659–70.

[10] Quoilin S, Orosz M, Hemond H, Lemort V. Performance and design optimization of a low-cost solar organic Rankine cycle. Solar Energy 2011;85(5):955–66.

[11] Invernizzi C, Bombarda P. Thermodynamic performance of selected HCFs for geothermal applications. Energy 1997;22(9):887–95.

[12] Hettiarachchi HDM, Golubovic M, Worek WM, Ikegami Y. Optimum design criteria for an organic Rankine cycle using low-temperature geothermal heat sources. Energy 2007;32:1698–706.

[13] Saleh B, Koglbauer G, Wendland M, Fischer J. Working fluids for low-temperature organic Rankine cycles. Appl Therm Eng 2011;31(14–15):2885–93.

[14] Shengjun Z, Huaixin W, Tao G. Performance comparison and parametric optimization of subcritical organic Rankine cycle (ORC) and transcritical

power cycle system for low-temperature geothermal power generation. Appl Energy 2011;88:2740–54.
[15] Guo T, Wang HX. Fluids and parameters optimization for a novel cogeneration system driven by low-temperature geothermal sources. Energy 2011;36(5):2639–49.
[16] Zhang FZ, Jiang PX. Thermodynamic analysis of a binary power cycle for different EGS geofluid temperatures. Appl Therm Eng 2012;48:476–85.
[17] Walraven D, Laenen B, D'haeseleer W. Comparison of thermodynamic cycles for power production from low-temperature geothermal heat sources. Energy Convers Manag 2013;66:220–33.
[18] Astolfi M, Xodo L, Romano MC, Macchi E. Technical and economical analysis of a solar–geothermal hybrid plant based on an organic Rankine cycle. Geothermics 2011;40(1):58–68.
[19] Saleh B, Koglbauer G, Wendland M, Fischer J. Working fluids for low-temperature organic Rankine cycles. Energy 2007;32:1210–21.
[20] Karellas S, Schuster A. Supercritical fluid parameters in organic rankine cycle applications. Int. J Thermodyn 2008;11(3):101–8.
[21] Guo T, Wang H, Zhang S. Comparative analysis of natural and conventional working fluids for use in transcritical Rankine cycle using low-temperature geothermal source. Int J Energy Res 2011:530–44.
[22] Preißinger M, Heberle F, Brüggemann D. Thermodynamic analysis of double-stage biomass fired organic Rankine cycle for micro-cogeneration. Int J Energy Res 2012;36(8):944–52.
[23] Borsukiewicz GA, Nowak W. Comparative analysis of natural and synthetic refrigerants in application to low temperature Clausius–Rankine cycle. Energy 2007;32(4):344–52.
[24] Chen H, Goswami DY, Rahman MM, Stefanakos EK. A supercritical Rankine cycle using zeotropic mixture working fluids for the conversion of low-grade heat into power. Energy 2011;36(1):549–55.
[25] Papadopoulos AI, Stijepovic MZ, Linke P. On the systematic design and selection of optimal working fluids for organic Rankine cycles. Appl Therm Eng 2010;30(6–7):760–9.
[26] Schuster A, Karellas S, Aumann R. Efficiency optimization potential in supercritical organic Rankine cycles. Energy 2010;35(2):1033–9.
[27] MATLAB version 7.8.0. Natick, Massachusetts: The MathWorks Inc; 2009.
[28] Lemmon EW, Huber ML, McLinden MO. NIST standard reference database 23: reference fluid thermodynamic and transport properties-REFPROP, version 9.0. Gaithersburg: National Institute of Standards and Technology, Standard Reference Data Program; 2010.
[29] Filippini S, Merlo U, Romano MC, Lozza G. Potential of water-sprayed condensers in ORC plantsIn First International Seminar on ORC Power Systems, Delft (NL); 22–23 September 2011.
[30] Di Pippo R. Ideal thermal efficiency for geothermal power plants. Geothermics 2007;36(3):276–85.